

## STUDY OF ERRORS OF A LASER OPTO-ACOUSTIC GAS ANALYZER

M. Sigrist, M.Yu. Kataev, A.A. Mitsel', Yu.N. Ponomarev, and A. Thony

*Institute of Atmospheric Optics,  
Siberian Branch of the Russian Academy of Sciences, Tomsk*

*Received July 7, 1994*

*The effect of different factors (accuracy in assigning a matrix of absorption coefficients, a model of water-vapor continuous absorption, and a random measuring error) on the accuracy of reconstructing the values of gas concentration from the data of opto-acoustic (OA) measurements is analyzed. The results of numerical simulation and processing of real signals of an OA gas analyzer with a CO<sub>2</sub> laser are presented.*

### 1. INTRODUCTION

Monitoring of gas composition of the atmospheric air by the optical absorption methods calls for instruments which are highly sensitive to absorption, highly selective, and capable of determining the concentration of trace gases in multicomponent mixtures. One of such instruments is an opto-acoustic (OA) gas analyzer with a resonance cell described elsewhere.<sup>1,2</sup> A radiation source is a CO<sub>2</sub> laser operating at a stable temperature of 20.5±0.1°C and generating 65–70 lines in the spectral range between 9.2 and 10.8 μm with 1–14 W radiant power.

To analyze the content of gases under study, an atmospheric air preliminary purified from atmospheric aerosol is pumped through the OA cell. The gas analyzer described enables one to identify simultaneously five gases: H<sub>2</sub>O, CO<sub>2</sub>, O<sub>3</sub>, NH<sub>3</sub>, and C<sub>2</sub>H<sub>4</sub>.

The problem on determining the gas concentration from OA signals is reduced to a solution of a system of linear algebraic equations (on the assumption of an optically thin layer in the OA cell)

$$y_i = \sum_{j=1}^m K_{ij} x_j + \alpha_c(\lambda_i), \quad i = 1, \dots, n, \quad (1)$$

where

$$y_i = U(\lambda_i) \cos(\theta_i) / (\eta P_0(\lambda_i)), \quad (2)$$

$U(\lambda_i)$  is the measured OA signal at the wavelength  $\lambda_i$ ,  $P_0(\lambda_i)$  is the laser radiative power at the same wavelength,  $\eta$  is the calibration constant of the OA gas analyzer,  $\theta_i$  is the phase shift between an incident flux of electromagnetic radiation and a signal from a microphone,  $K_{ij}$  is the absorption coefficient of the  $j$ th gas at the wavelength  $\lambda_i$ ,  $x_j$  is the concentration of the  $j$ th gas, and  $\alpha_c(\lambda_i)$  is the coefficient of water vapor continuous absorption. In expression (1) we take into account the effect of kinetic cooling; therefore, the term responsible for absorption due to carbon dioxide has the form<sup>1</sup>

$$(1 - v_{N_2}(V_1) / (10^4 / (\lambda_i))) K_{iCO_2} x_{CO_2}, \quad (3)$$

where  $v_{N_2}$  is the frequency of vibrational mode  $V_1$  of the N<sub>2</sub> molecule being equal to 2330 cm<sup>-1</sup>.

Our work is aimed at studying the accuracy of gas concentration reconstruction from OA measurements depending on: (a) error in determining the absorption coefficients  $K_{ij}$ ; (b) available model of continuous absorption  $\alpha_c(\lambda_i)$ ; (c) random error in measuring signals. To analyze the aforementioned errors, we must solve the inverse problem

$$x = (K^T W K)^{-1} K^T W y, \quad (4)$$

where  $y$  is the  $n$ -dimensional vector consisting of the elements  $(y_i - \alpha_c(\lambda_i, \rho_{H_2O}^0))$ ;  $K$  is the  $(n \times m)$  matrix of the system, whose elements are the absorption coefficients  $K_{ij}$ ;  $x$  is the  $m$ -dimensional vector of the unknown values of concentration; and,  $W$  is the  $(n \times m)$  diagonal matrix of weight factors.

In the solution of the inverse problem, the column of the  $K$  matrix responsible for water vapor was formed taking into account the square-law  $\alpha_c$  dependence on water vapor concentration, i.e.,

$$K_{iH_2O} = K_{iH_2O} + d_1(\lambda_i) + 2 d_2(\lambda_i) \rho_{H_2O}^0,$$

where  $\rho_{H_2O}^0$  is the initial approximation for H<sub>2</sub>O concentration, and  $d_1(\lambda_i)$  and  $d_2(\lambda_i)$  are the coefficients of linear and quadratic terms in  $\alpha_c$ .

### 2. ABSORPTION COEFFICIENTS OF THE SYSTEM MATRIX

Table I lists the absorption coefficients calculated using the LARA package<sup>3</sup> based on the HITRAN-91 atlas.<sup>4</sup> Given in Table II are the experimental results from different publications. Without discussing the cause of disagreement between the absorption coefficients in Tables I and II as well as the accuracy of experimental results, we intend to study the errors in determining the gas concentration using an inadequate matrix. It should be noted that the absorption coefficients of H<sub>2</sub>O, O<sub>3</sub>, NH<sub>3</sub>, and C<sub>2</sub>H<sub>4</sub> in Table II are overestimated and the absorption coefficient of CO<sub>2</sub> is underestimated as compared to those in Table I.

TABLE I. Absorption coefficients ( $\text{cm}^{-1} \text{atm}^{-1}$ ) for five gases calculated from the HITRAN–91 data.

Transition	Frequency, $\text{cm}^{-1}$	H <sub>2</sub> O	CO <sub>2</sub>	O <sub>3</sub>	NH <sub>3</sub>	C <sub>2</sub> H <sub>4</sub> *
9P34	1033.488	0.106e–5	0.146e–2	0.317e+1	0.307e+1	0.200e+1
9P26	1041.279	0.107e–5	0.279e–2	0.519e+1	0.481e–1	0.260e–0
9P24	1043.163	0.144e–5	0.311e–2	0.621e–0	0.221e–0	0.420e–0
9P14	1052.196	0.429e–5	0.332e–2	0.119e+2	0.276e–0	0.150e–0
9R30	1084.635	0.301e–5	0.235e–2	0.832e–1	0.773e+2	0.150e–0
10P34	931.001	0.300e–6	0.105e–2	0.802e–4	0.112e+2	0.170e+1
10P20	944.194	0.489e–5	0.251e–2	0.765e–3	0.545e–1	0.210e+1
10P14	949.479	0.344e–5	0.235e–2	0.173e–2	0.404e–0	0.320e+2
10R20	975.930	0.742e–3	0.270e–2	0.106e–0	0.383e–2	0.130e+1
10R34	984.383	0.810e–5	0.112e–2	0.200e–0	0.259e–3	0.770e–0

\*Absorption coefficients of C<sub>2</sub>H<sub>4</sub> are borrowed from Ref. 1.

TABLE II. Absorption coefficients ( $\text{cm}^{-1} \text{atm}^{-1}$ ) for five gases borrowed from different literature sources.

Transition	Frequency, $\text{cm}^{-1}$	H <sub>2</sub> O (Ref. 5)	CO <sub>2</sub> (Ref. 1)	O <sub>3</sub> (Ref. 6)	NH <sub>3</sub> (Ref. 7)	C <sub>2</sub> H <sub>4</sub> (Ref. 7)
9P34	1033.488	0.810e–4	0.110e–2	0.360e+1	0.400e+1	0.200e+1
9P26	1041.279	0.650e–4	0.250e–2	0.590e+1	0.125e–0	0.225e–0
9P24	1043.163	0.820e–4	0.270e–2	0.830e+0	0.500e–0	0.400e–0
9P14	1052.196	0.930e–4	0.320e–2	0.124e+2	0.400e–0	0.145e–0
9R30	1084.635	0.130e–3	0.170e–2	0.173e–0	0.750e+2	0.187e–0
10P34	931.001	0.840e–4	0.950e–3	0.028e–0	0.137e+2	0.175e+1
10P20	944.194	0.910e–4	0.220e–2	0.027e–0	0.200e–0	0.225e+1
10P14	949.479	0.850e–4	0.180e–2	0.029e–0	0.950e–0	0.375e+2
10R20	975.930	0.800e–3	0.210e–2	0.148e–0	0.550e–1	0.120e+1
10R34	984.383	0.500e–4	0.750e–3	0.250e–0	0.110e–1	0.890e+0

### 3. MODELS OF CONTINUOUS ABSORPTION FOR THE ATMOSPHERIC 8–12 $\mu\text{m}$ WINDOW

The continuous absorption coefficient  $\alpha_c$  entering into Eq. (1) depends on pressure, temperature, humidity, and wavelength. To solve the system of equations (1) or (4), it is necessary to know the analytical dependence of  $\alpha_c$  on the aforementioned parameters, i.e., we must have a model of water vapor continuous absorption.

The problem of radiation absorption in the 8–12  $\mu\text{m}$  window was posed almost a century ago.<sup>8</sup> Both theoretical and experimental works were devoted to studying the patterns of optical radiation absorption. An overview of the state-of-the-art studies of continuous absorption is given in Refs. 8 and 9. Without dwelling on the nature of this phenomenon, note its specific features: negative temperature dependence (for a temperature range realized in the atmosphere) and the square-law dependence on the water vapor concentration.

To construct an efficient calculational scheme for solving the inverse problem (4), it is necessary

to use the models of continuous absorption that meet the following requirements: (a) reproduce the complete patterns occurring in the real atmosphere; (b) are rather simple in numerical realization; (c) result in no unjustified complication of the algorithm for solving the inverse problem. Empirical models fit these requirements.

By the present time two models of continuous absorption: the model of Roberts et al.<sup>10</sup> and the model of Aref'ev<sup>8</sup> are most widely used. In addition to these models, we consider the model constructed at the Institute of Atmospheric Optics.<sup>11</sup> Table III lists the comparison results for the coefficients  $\alpha_c$  calculated using the foregoing models. Presented here too are the results for  $\alpha_c$  obtained using the model written in the computer code LOWTRAN–7 (see Ref. 12). The largest discrepancy in the absorption coefficients  $\alpha_c$  is observed for models from Refs. 10 and 11 (see Table III). It attains 22% (at  $\rho = 1 \text{ g/m}^3$ ) and increases with increasing humidity up to 27% (at  $\rho = 15 \text{ g/m}^3$ ).

TABLE III. Continuous absorption coefficient  $\alpha_c$ , in  $\text{km}^{-1}$  ( $\lambda = 10.591 \mu\text{m}$ ,  $T = 293 \text{ K}$ , and  $P = 1 \text{ atm}$ ).

$\rho, \text{g/m}^3$	$\alpha_c, \text{km}^{-1}$			
	Ref. 10	Ref. 8	Ref. 11	LOWTRAN–7
1	$5.05 \cdot 10^{-3}$	$4.20 \cdot 10^{-3}$	$3.91 \cdot 10^{-3}$	$1.70 \cdot 10^{-3}$
5	$4.65 \cdot 10^{-2}$	$3.99 \cdot 10^{-2}$	$3.48 \cdot 10^{-2}$	$2.71 \cdot 10^{-2}$
10	$1.46 \cdot 10^{-1}$	$1.27 \cdot 10^{-1}$	$1.07 \cdot 10^{-1}$	$9.80 \cdot 10^{-1}$
15	$2.99 \cdot 10^{-1}$	$2.62 \cdot 10^{-1}$	$2.18 \cdot 10^{-1}$	$2.19 \cdot 10^{-1}$

The comparison of the results of investigation of the H<sub>2</sub>O absorption in the 8–12 μm window published for 20-year period with those obtained using the computer codes LOWTRAN–7 and HITRAN was performed in Ref. 9. The agreement between the calculated values and the most representative experimental data was shown to be sufficiently good.

Listed in the last column of Table III are the values α<sub>c</sub> calculated using the code LOWTRAN–7. Of three models borrowed from Refs. 10, 8, and 11, the closest to LOWTRAN–7 is the model borrowed from Ref. 11. The disagreement between this model and LOWTRAN–7 at low humidity (ρ = 1 g/m<sup>3</sup>) is 100%; with the humidity increase, it decreases rapidly and falls to 1–2% at ρ = 15 g/m<sup>3</sup>. In Section 4 we show the distortions in the results of the inverse problem solution that are obtained for an inadequate model of continuous absorption.

**4. SIMULATION OF THE INVERSE PROBLEM**

**4.1 Effect of measuring error on the inverse problem solution accuracy**

The numerical experiment was carried out according to a closed scheme. The elements y<sub>i</sub> were calculated from the specified values of gas concentration listed in Table IV (see x<sub>true</sub>) and the absorption coefficients taken from Table I. The coefficient α<sub>c</sub> was calculated for the model from Ref. 11 and added to the elements y<sub>i</sub>. The values y<sub>i</sub> thus obtained were distorted with random numbers ε<sub>i</sub> (ỹ<sub>i</sub> = y<sub>i</sub> + ε<sub>i</sub>) to imitate the measurement noise. Then the inverse problem was solved and the elements of the vector x<sub>j</sub> (values of gas concentration) were determined. To find the manner in which the random measuring error affects the values of gas concentration obtained by solving the inverse problem, we simulated random realization of vectors y, and the concentration vector x was calculated for each realization. Figure 1 a depicts the values of gas concentration (components of the vector x<sub>j</sub>) vs. the serial number of realization for a noise level of 10%. As seen from Fig. 1 a, the strongest variations of the reconstructed values of gas

concentration are observed for O<sub>3</sub> (up to 27), CO<sub>2</sub> (up to 19), and C<sub>2</sub>H<sub>4</sub> (up to 17%). Concentration deviations from the initial value are no larger than 16 and 10% for water vapor and ammonia, respectively.

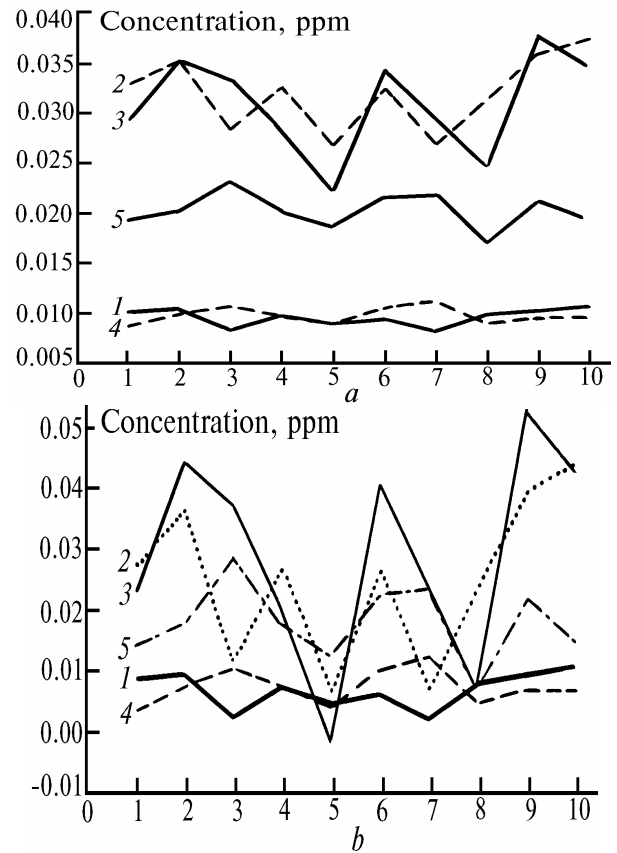


FIG. 1. Effect of the error in measuring the OA signal on the accuracy of reconstructing the gas concentration for ε = 10 (a) and 40% (b). The serial numbers of random realization of the vector y are plotted on the abscissa. The calculations were performed for H<sub>2</sub>O (1), CO<sub>2</sub> (2), O<sub>3</sub> (3), NH<sub>3</sub> (4), and C<sub>2</sub>H<sub>4</sub> (5).

TABLE IV. Inverse problem solution.

Gas	x <sub>true</sub> , ppm	x(1), ppm	x(2), ppm	x(3), ppm	x(4), ppm
H <sub>2</sub> O	1.00·10 <sup>4</sup>	1.00·10 <sup>4</sup>	9.98·10 <sup>3</sup>	9.81·10 <sup>3</sup>	9.73·10 <sup>3</sup>
CO <sub>2</sub>	330	330	381	365	416
O <sub>3</sub>	3.0·10 <sup>-2</sup>	3.0·10 <sup>-2</sup>	3.4·10 <sup>-2</sup>	3.6·10 <sup>-2</sup>	3.9·10 <sup>-2</sup>
NH <sub>3</sub>	1.0·10 <sup>-2</sup>	1.0·10 <sup>-2</sup>	9.7·10 <sup>-3</sup>	8.6·10 <sup>-3</sup>	7.9·10 <sup>-3</sup>
C <sub>2</sub> H <sub>4</sub>	2.0·10 <sup>-2</sup>	2.0·10 <sup>-2</sup>	1.9·10 <sup>-2</sup>	1.4·10 <sup>-2</sup>	1.2·10 <sup>-2</sup>

With the increase in the measurement noise level, the solution starts to oscillate. Figure 1 b shows the results of solution of the inverse problem for a measuring error of 40%. Here the ozone concentration oscillations attain 100% and larger. There appear even negative values. For CO<sub>2</sub>, the largest concentration deviation from the initial one is about 75%; for C<sub>2</sub>H<sub>4</sub>, H<sub>2</sub>O, and NH<sub>3</sub> they are 68, 63, and 51%, respectively.

**4.2 Effect of the accuracy in assigning the system matrix K and the continuous absorption model on the inverse problem solution**

Consider now the effect of the accuracy in assigning the absorption coefficient matrix and the continuous absorption model on the results of solution of the inverse problem. Simulation was carried out in the following manner. As in paragraph 4.1, we calculated the y–vector

elements from the tabulated data on the  $K$  matrix (see Table I) and the continuous absorption model from Ref. 11. The inverse problem was then solved.

Four versions of the inverse problem solution were treated: (1) the solution  $x(1)$  obtained for the matrix  $K$  and coefficient  $\alpha_c$  that were used in calculation of the  $y$ -vector elements (i.e.,  $K$  was taken from Table I and  $\alpha_c$  – from Ref. 11); (2) the solution  $x(2)$  obtained for the matrix  $K$  (Table I) but for the other model of the coefficient  $\alpha_c$  taken from Ref. 10; (3) the solution  $x(3)$  obtained for the other matrix  $K$  (see Table II) and the initial model of the coefficient  $\alpha_c$  (see Ref. 11); and, (4) the solution  $x(4)$  obtained for the other matrix  $K$  and the other model of the coefficient  $\alpha_c$  (see Ref. 10).

The effect of the error in the continuous absorption model on the reconstructed values of gas concentration is shown in the column  $x(2)$  of Table IV. The largest distortion is observed for  $\text{CO}_2$  ( $\approx 15\%$ ) and  $\text{O}_3$  (13%). It should be noted that the concentration of both gases increases. The smallest distortion is found for  $\text{H}_2\text{O}$  (0.2%). The increase in  $\text{CO}_2$  concentration for inadequate model of  $\alpha_c$  from Ref. 10 ( $\alpha_c$  from Ref. 10 is larger than  $\alpha_c$  from Ref. 11) is accounted for by the fact that  $\text{CO}_2$  absorption is subtracted from the total absorption (the effect of kinetic cooling in a resonance cell of opto-acoustic converter); therefore, the  $\text{CO}_2$  concentration increases with the increase in  $\text{H}_2\text{O}$  concentration or absorption coefficients.

The column  $x(3)$  demonstrates the effect of the system matrix accuracy on the solution. Here we also observe 11 and 20% increase in the values of  $\text{CO}_2$  and  $\text{O}_3$  concentration and 14 and 32% decrease in the values of  $\text{NH}_3$  and  $\text{C}_2\text{H}_4$  concentration. Overestimated  $\text{CO}_2$  concentration in  $x(3)$  is caused by two factors. First, the absorption coefficients of  $\text{H}_2\text{O}$  and  $\text{CO}_2$  for inadequate model of the system matrix (compare Tables I and II) are overestimated in comparison with the initial matrix. Second, the effect of kinetic cooling is also observed here. The decrease in  $\text{NH}_3$  concentration is accounted for by the increase in the  $\text{NH}_3$  absorption for inadequate matrix. The decrease in the values of the  $\text{C}_2\text{H}_4$  and  $\text{H}_2\text{O}$  concentration can be explained in the same way. The increase in ozone concentration is due to an internal property of system matrix (4). The effect of the two factors: inadequate matrix and inadequate model of continuous  $\text{H}_2\text{O}$  absorption is seen from the solution  $x(4)$ . Here the values of  $\text{CO}_2$  and  $\text{O}_3$  concentration increase by 26 and 32% and the values of  $\text{NH}_3$  and  $\text{C}_2\text{H}_4$  concentration decrease by 20 and 40%, respectively. The  $\text{H}_2\text{O}$  concentration, as in the previous cases, varies only slightly ( $< 1\%$ ).

## 5. PROCESSING OF REAL DATA OF AN OA GAS ANALYZER

Let us consider the results of processing of the real data obtained with an OA gas analyzer based on a  $\text{CO}_2$  laser with a resonance cell. The system was described at length in Refs. 1 and 2. The laser transitions (9P34, 9P26, 9P24, 9P14, 9R30, 10P34, 10P20, 10P14, 10R20, and 10R34) used here provided simultaneous

determination of  $\text{H}_2\text{O}$ ,  $\text{CO}_2$ ,  $\text{O}_3$ ,  $\text{NH}_3$ , and  $\text{C}_2\text{H}_4$  concentration. During the experiment, we also measured air temperature, pressure, and humidity. The diurnal experimental data were obtained in Morschach (Central Switzerland) on July 26, 1990.

The absorption coefficients listed in Table I were used for processing of the experimental results. By way of example, Fig. 2 depicts the reconstructed values of the  $\text{CO}_2$  concentration for two models of continuous absorption.<sup>10,11</sup> As seen from Fig. 2, the difference between the values of  $\text{CO}_2$  concentration varies from 60 to 120 ppm for different models of  $\alpha_c$ .

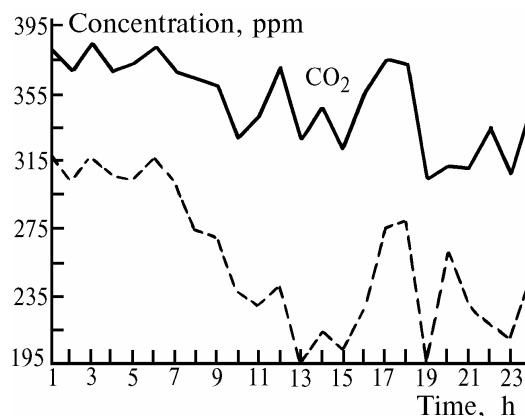


FIG. 2. Processing of real data of the OA measurements (July 26, 1990, Switzerland): solid line is for the model  $\alpha_c$  from Ref. 10 and dashed line is for the model  $\alpha_c$  of the Institute of Atmospheric Optics (see Ref. 11).

## REFERENCES

1. P.L. Meyer and M.W. Sigrist, Final Report SNE/NFP 14, Project No. 4.684.083.14, Zurich, 1988.
2. A. Thöny, "New development in  $\text{CO}_2$ -laser photoacoustics of trace gases," Diss. ETH No. 10345, Swiss Federal Institute of Technology, Zurich (1994).
3. A.A. Mitsel' and V.P. Rudenko, "Software package LARA-1 (version 1986) for calculating the energy losses of laser radiation in the atmosphere," Preprint No. 57, Tomsk Affiliate of the Siberian Branch of the Academy of Sciences of the USSR, Tomsk (1988).
4. L.S. Rothman, R.R. Gamache, R.H. Tipping, et al., J. Quant. Spectrosc. Radiat. Transfer **48**, 469–507 (1992).
5. J. Hinderling, M.W. Sigrist, and F.K. Kneubühl, Infrared Phys. **27**, 63–120 (1987).
6. F.J.M. Harren, "The photoacoustic effect, refined and applied to biological problems," Proefschrift, Krips repro Meppel, 1988.
7. J. Boshier, G. Schäfer, and W. Wiesemann, Report BF-R-63.616-4, Batelle Institute, Frankfurt, 1979.
8. V.N. Aref'ev, Atm. Opt. **2**, No. 10, 878–894 (1989).
9. W. Grant, Appl. Opt. **29**, No. 4, 451–462 (1990).
10. R.E. Roberts, J.E.A. Selby, and L.M. Biberman, Appl. Opt. **15**, No. 9, 2085–2090 (1976).
11. N.N. Shchelkanov, Yu.A. Pkhalagov, and V.N. Uzhegov, Atmos. Oceanic Opt. **5**, No. 7, 431–434 (1992).
12. L.W. Abreu, F.X. Kneizys, G.P. Anderson, and J.H. Chetwynd, in: *Proceedings of the 14th Conference on Atmospheric Transmittance Models*, Hanscom AFB (1991), pp. 65–72.